



## General procedure for selecting and testing materials and coatings in response to a tribological problem

Julie Pellier, Jean-Yves Paris, Jean Denape, Joël Bry, Vincent Genissieux

### ► To cite this version:

Julie Pellier, Jean-Yves Paris, Jean Denape, Joël Bry, Vincent Genissieux. General procedure for selecting and testing materials and coatings in response to a tribological problem. *Journal of Tribology*, 2017, 139 (3), pp.0. 10.1115/1.4034331 . hal-01905418

**HAL Id: hal-01905418**

**<https://hal.science/hal-01905418>**

Submitted on 25 Oct 2018

**HAL** is a multi-disciplinary open access archive for the deposit and dissemination of scientific research documents, whether they are published or not. The documents may come from teaching and research institutions in France or abroad, or from public or private research centers.

L'archive ouverte pluridisciplinaire **HAL**, est destinée au dépôt et à la diffusion de documents scientifiques de niveau recherche, publiés ou non, émanant des établissements d'enseignement et de recherche français ou étrangers, des laboratoires publics ou privés.






## Open Archive Toulouse Archive Ouverte

OATAO is an open access repository that collects the work of Toulouse researchers and makes it freely available over the web where possible

This is an author's version published in: <http://oatao.univ-toulouse.fr/19727>

**Official URL:** <http://doi.org/10.1115/1.4034331>

**To cite this version :**

Pellier, Julie  and Paris, Jean-Yves  and Denape, Jean  and Bry, Joël and Genissieux, Vincent *General procedure for selecting and testing materials and coatings in response to a tribological problem.* (2016) Journal of Tribology, 139. ISSN 0742-4787

Any correspondence concerning this service should be sent to the repository administrator: [tech-oatao@listes-diff.inp-toulouse.fr](mailto:tech-oatao@listes-diff.inp-toulouse.fr)

**Julie Pellier**

Laboratoire Génie de Production (LGP),  
Université de Toulouse,  
INP-ENIT,  
47, Avenue d'Azereix,  
B.P. 1629,  
Tarbes Cedex 65016, France

**Jean-Yves Paris<sup>1</sup>**

Laboratoire Génie de Production (LGP),  
Université de Toulouse,  
INP-ENIT,  
47, Avenue d'Azereix,  
B.P. 1629,  
Tarbes Cedex 65016, France  
e-mail: jean-yves.paris@enit.fr

**Jean Denape**

Laboratoire Génie de Production (LGP),  
Université de Toulouse,  
INP-ENIT,  
47, Avenue d'Azereix, B.P. 1629,  
Tarbes Cedex 65016, France  
e-mail: jean.denape@enit.fr

**Joël Bry**

AEREM,  
18 Avenue du Louron,  
Colomiers 31770, France  
e-mail: joel.bry@aerem.fr

**Vincent Genissieux**

PULSWER S.A.,  
8 Boulevard Roger Salengro,  
Grenoble 38100, France  
e-mail: vincent.genissieux@pulswer.com

# General Procedure for Selecting and Testing Materials and Coatings in Response to a Tribological Problem

*In general, there is no available tool which can help engineers and researchers to choose optimal materials for friction pairs. This article proposes a dual approach for the choice of materials and coatings. First, in order to select the initial materials, a selection matrix helps to rank a reduced number of solutions to a tribological problem with the aim of building the most credible and viable experimental campaign. Then, this experimental phase is necessary for final selection taking into account tribological properties. The final step involves experimental validation on a prototype and on the real device. This methodology was applied on the complex geometry of an air compressor under severe friction conditions. Technical specifications are defined by a functional analysis of the tribological system. Then, the selection matrix is created on the basis of empirical rules and bibliographic data, including predetermined material/coating properties, process considerations, and tribological features, in accordance with the functional analysis. As an example, four potential solutions were tested: diamondlike carbon (DLC) and polytetrafluoroethylene (PTFE) coatings on 15-5PH stainless steel and two composites, reinforced PTFE and polyetheretherketone (PEEK). Experimental results were then compared to expected values from the specifications. The performance of each solution was highlighted by a graphic radar representation. The selection matrix gave the DLC coatings as one of the best solutions, and experimental tests confirmed this choice while allowing to refine the preselected solutions. This result shows that the selection matrix gives a reliable choice of optimal solutions. [DOI: 10.1115/1.4034331]*

**Keywords:** tribology application, choice methodology, selection matrix, graphic radar, optimal material pairs, air compressor

## 1 Introduction

Friction and wear are two major problems in many industrial applications especially for parts in poorly lubricated systems or in dry conditions. Choosing and selecting the optimal friction couple are essential for resolving such problems. A large number of materials are used to meet these tribological requirements. They can be divided into *bulk materials*, such as graphite [1], cast iron [2], bronze alloys [3], beryllium copper alloys [4], ceramics [5], or even polymers [6], and *surface coatings*, such as hard coatings [7,8], solid lubricant coatings [9], among others. All these solutions may control friction and prevent wear, but only in specific conditions. However, engineers have to keep in mind that wear resistance is a systemic property which depends on operating conditions and contact life (interfacial elements behavior). This means that a satisfactory performance for given conditions may be inadequate for a seemingly identical case.

The most secure approach to deal with any tribological study is based on the concept of tribological triplet [10]. It takes into consideration friction and wear phenomena according to three distinct levels:

- The *working system*, which is the real engine or experimental device, imposes the entirety of the contact stresses, such as

load, sliding conditions (continuous or reciprocating motion, speed, and frequency) and environment.

- The *first bodies* which describe the two materials which are in contact and create the working conditions.
- The *third body* which identifies the interfacial elements, such as lubricant, contaminants, or debris, still presents between the two first bodies.

The role of each level is decisive, and attention should not exclusively focus on the material level, i.e., the *first bodies*. Therefore, the *working system*, and in particular its stiffness must not be neglected. This suggests that all the tribological tests performed at the laboratory scale using a specific tribometer must be validated with tests on a prototype device and then on the real device to guarantee the reliability of the solution. Furthermore, the circulation of the *third body* contributes to the load-carrying capacity of the contact by assuming the major amount of the speed accommodation between the two rubbing materials. This level, therefore, also needs to be given serious consideration.

From an industrial point of view and considering the lack of general predictive models, it is well known that experimental tests of all the available solutions (bulk materials and surface coatings) are not easy to implement, are overpriced, and would require a great deal of unnecessary time. To avoid a vast number of experimental tests, it would be better to find a way to propose a reduced number of solutions and then to refine this preselection by experimental tests. However, currently there are no general guidelines to help with the initial selection because [11]:

<sup>1</sup>Corresponding author.

- The durability of bulk materials or surface coatings depends on a large number of parameters;
- Wear mechanisms are supposed to help in the selection but in most cases, the material loss is the result of various successive or concurrent wear mechanisms;
- Engineers and even tribologists may not often be aware enough of third body formation and rheology; and
- The literature has to be considered with extreme caution because every change in tribological parameters (contact geometry and sliding conditions) or solutions for the coatings process (example for DLC coatings [12]) could lead to very different responses.

The aim of this study is to propose a general procedure for selecting and testing materials and coatings when confronting a tribological problem. We will begin with a bibliographical review of existing methods of materials selection.

## 2 Bibliographical Review and Proposed Approach

**2.1 Methods for Materials/Coatings Selection.** Several methods exist for selecting materials or coatings. Brechet et al. [13] developed a general multicriteria and multidesign elements analysis of the selection of materials, organized as an extension of Ashby's method. It should be noted that this method does not index the coatings.

However, no specific method of materials selection was developed which take friction into consideration. The major problem with the usual approaches comes from the fact that, in mechanical engineering, the choice of materials is usually made based on intrinsic properties (essentially, volume properties which are easily accessible), while, in tribology, the choice of materials involves a large number of interactive parameters (such as surface and interface properties, which are often unknown) and also includes the behavior of the working system, as mentioned previously. In this case, only empirical rules can be applied for deciding what friction pairs may be chosen [14], such as:

- Promote the *friction compatibility* by choosing a pair of materials with insoluble (chemically nonmiscible) features to prevent seizure (i.e., avoid homogeneous contacts, in particular when involving metallic materials), while also taking into account the risk of galvanic cell;
- Ensure the *mechanical accommodation* (deformation ability and resistance to penetration) of the sliding pair by selecting the material with the lowest Young's modulus (or the lowest hardness) for the smallest moving surface;
- Limit *abrasion risks* by assigning the lowest roughness to the hardest material;
- Limit the *extension of adhesive junctions* by orienting the machining grooves in the opposite direction to the movement;
- Favor *surface roughness* characterized by a negative skewness to improve lubricant or debris retention;
- Strengthen *superficial layers* by surface treatments (mechanical, conversion, or diffusion treatments) or coating deposits, while avoiding property gradients which are too large, in order to prevent further delamination wear; and
- Choose a high *thermal conductivity* for the material with the largest moving surface, as this will dissipate heat more easily, reduce the contact temperature, and avoid the risk of overheating.

Such rules are often necessary but never sufficient. In the absence of predictive models, experiments are still required to evaluate the contact integrity under the most realistic conditions possible. In addition, the results cannot be extrapolated to other situations without careful consideration. However, some methodologies have been proposed for the selection of surface treatments.

Dobrzanski and Madejski [15] proposed an expert system for selecting the best coating, depending on the application and the

working conditions. They used a large number of factors associated with relevant weights. The method presented was tested on a specific application and was found to work properly. However, the limitations of this procedure are such that it is only applicable to metallic coatings. It also needs more specifications for the deposition process as this method does not work for specific tribological studies. Other expert systems exist based on the same procedure [16–19].

Schiffmann et al. [20] developed an innovative web-based information system (INO) for coatings. It should enable engineers to make a preselection about the kind of coating that may be needed for a specific surface problem and then should lead to a solution for the choice of optimized products.

Matthews et al. [21,22] also developed an interesting methodology for coating selection based on the best compromise between "what is needed" and "what is possible." Nine steps are described in Ref. [21], which briefly contain:

- application and design study, i.e., identification of critical tribological elements
- component specification, i.e., detailed analysis of tribological elements
- functional tribological requirements, i.e., vibrations and admissible wear
- substrate surface requirements, i.e., coating thickness and hardness
- nonfunctional requirements, i.e., maximum weight and dimension for coating and masking
- economic and procurement requirements, i.e., costs, delivery time, and environmental constraints
- coating process characteristics, i.e., process temperature, precision of thickness, and roughness change
- coating material properties, i.e., properties independent of the process
- specific coating material and process characteristics, i.e., a combination of the two previous steps

This methodology takes into account many tribological features, material, coating, and process parameters and enhances the key points needed for a tribological system to work well. It is a reliable approach to tell whether or not a particular coating can be used, however, it does not give them a ranking.

**2.2 Methods Based on Experimental Phases to Classify Solutions.** Other tools derive from experimental studies and tribological performances of coatings under specific conditions, especially for fretting conditions [23,24]. They can be divided into three groups:

- Coatings are tested and then compared to a reference solution used in the same conditions. Wöhler-like curves (maximal contact pressure versus coating lifetime) can be used to compare different coatings [25].
- A performance index can also be introduced: a parameter  $P$  (for example, coefficient of friction, wear, or durability) of a tested coating  $x$  is compared to a reference coating  $r$ . Then, the performance index  $I$  can be calculated for the coating  $x$  as  $I_x = P_r/P_x$ . If  $I_x < 1$ , the coating  $x$  provides a better solution than reference  $r$  [23].
- Polar diagrams give another accurate visual representation, used to find the best coatings after friction tests [26]. The major parameters of the tribological system are divided into four categories: intrinsic properties of the coatings, coating–substrate interaction, running conditions, and material response. The results for each coating are compared with the reference (uncoated solution) and are plotted using a polar diagram.

These experimental approaches offer different ways of structuring results and different visual representations of the performance of a tribological solution, but an experimental reference is necessary for the comparison.

**2.3 Proposed Procedure for Selecting and Testing Materials and Coatings.** Our aim is to propose a selection method when faced with a tribological problem, for choosing the first bodies. This method involves proposing a reduced number of solutions in order to build the most credible and viable experimental campaign (Fig. 1). Then, the experimental phase allows for final selection taking into account tribological properties.

This strategy requires a prior *functional analysis of the contact* of the real tribological system. This should be as complete as possible. The analysis defines the technical specifications through operational and environmental parameters. Materials parameters are empirically chosen at this point and are introduced, in accordance with technical specifications, to build the *materials selection matrix*. Solutions selected from the material matrix are given grades in order to give structure to the choices. Then, an *experimental phase* allows to refine the preselected solutions. Using the matrix, the first experimental phase on a laboratory tribometer (with simplified geometries and ideal operating conditions) is shorter and more effective. So, a reduced number of solutions is tested on a prototype device (under the most realistic conditions possible). The final experimental phase on the real device provides the best solution.

If laboratory or prototype tests lead to insufficient performances of the materials, a new investigation of the materials matrix is required. Moreover, if laboratory or prototype tests lead to materials failure, modifications of the design or of the operating conditions may be considered.

In the following sections, a functional analysis of a contact is first set out in detail (Sec. 3) followed by the establishment and the use of the materials selection matrix (Sec. 4), and finally, some results of the experimental tests are presented (Sec. 5).

### 3 First Phase: Functional Analysis of the Contact

A realistic functional analysis has to consider three steps:

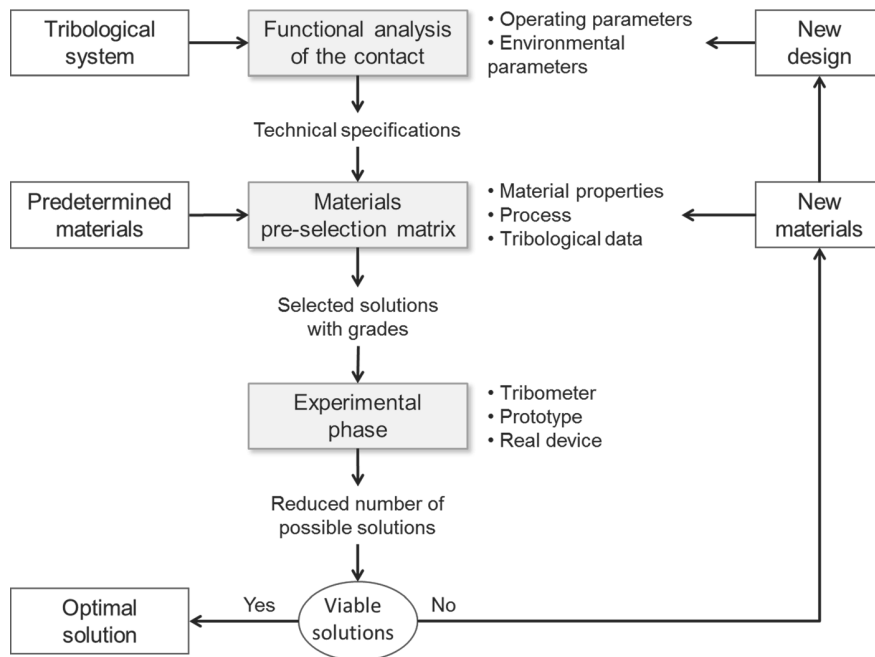
- The first step defines the explicit functions the contact will perform in addition to friction, like corrosion, impact, or fatigue resistance.

- The second step specifies the tribological operating parameters including operational and environmental parameters (Table 1). This defines the technical specifications.
- The last step ranks the parameters in order of priority, disregards those that can be overlooked, and then simplifies the others for laboratory tests.

The method of materials/coatings selection was developed for a specific device: an air compressor with variable volume chambers (Fig. 2(a)) defined between an ovoid shape stator and a deformable four-piston kinematic chain rotor. This kind of compressor is a rotational device where several contacts can be identified. The most sensitive friction problem is located on the linear contact. The complex industrial geometry of this contact has been simplified to promote a linear contact composed of a cylindrical bar on a cylindrical-shaped sample (Fig. 2(b)).

The tribological parameters of this application are collected in Table 2. Operational and environmental parameters are listed for the device. These contact conditions are a result of averages based on estimated or numerically computed values established from the study of the real-life conditions. For instance, different pressures are applied according to the materials used because numerical analysis gives a different pressure response when polymers or metals are involved. Afterward, some of these parameters must be simplified for tribometer tests. For example, only one mean contact pressure is applied: 6 MPa for massive polymer-steel contacts and of 15 MPa for coatings-coatings contacts.

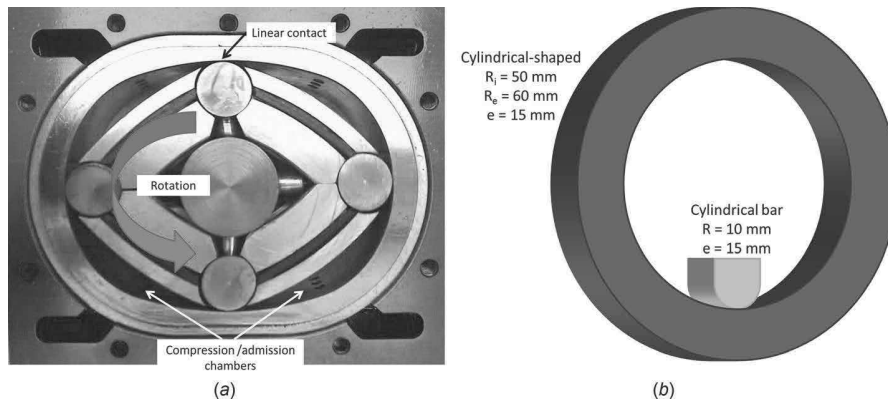
The objectives of this study are to find optimal frictional couples, relating to specifications described in Fig. 2 and Table 2. The contact must lead to minimal debris generation, resist corrosion, and have “good behavior during friction,” i.e., the coefficient of friction and the life duration of the contact must be inferior/superior to a threshold value. Many material solutions can be proposed: either bulk materials or surface coatings. For surface coatings, no specific substrates are preselected. The substrate will be chosen for two reasons: because it satisfies the specifications, and also because it is the best solution for the selected coatings in terms of adhesion resistance and hardness ratio. The behavior of surface coatings largely depends on the substrate properties.



**Fig. 1 Problem summary: How to find a reduced number of solutions in response to a tribological problem?**

**Table 1 Main parameters to be taken into account for a tribological problem according to Ref. [27]**

Operational parameters	Friction mode	Rolling, sliding (reciprocating, rotary, and oscillating), and fretting
	Contact geometry	Dimensions, surface shape, Hertzian or not, open or closed, conformal or not, and clearance
	Bodies assignment	Size of moving surfaces
	Contact mechanics	Contact pressure or load, sliding speed, frequency, temperature, time running, number of cycles, and displacement amplitude
Environmental parameters	Device	Stiffness, natural frequency, inertia, and damping
	Atmosphere	Oxidizing or reducing environment, vacuum, partial pressures, humidity, and contaminant
	Type of lubrication	Solid, liquid, gaseous, and none
	Mode of lubrication	Hydrostatic, hydrodynamic, and limit

**Fig. 2 (a) Air compressor where a deformable four-piston kinematic chain rotor rotates inside a fixed ovoid shape stator leading to the volume variation of compression/admission chambers and (b) modeling of the contact geometry which is a linear contact****Table 2 Operational and environmental parameters of the case study**

		Actual device	Tribometer
Operational parameters	Friction mode	Continuous sliding and rotatory	Continuous sliding and rotatory
	Contact geometry	Hertzian, with change in contact width (open contact)	Hertzian (open contact)
	Contact mechanics	Variable contact pressure: from 2 to 15 MPa (numeric calculus)	Constant contact pressure: 6 MPa or 15 MPa (depends on the selected material)
		Variable sliding speed: from 5 to 8 m s <sup>-1</sup>	Constant sliding speed: 8 m s <sup>-1</sup>
		Frequency: from 25 to 100 Hz	Frequency: 25 Hz
Environmental parameters	Device	Variable temperature depending on compression and friction: from 150 to 250 °C (numeric calculus)	Constant temperature: 150 °C (environmental temperature)
		Time running > 1000 h	Time running = 2 h
		Air compressor	Specially designed and manufactured for this study
		Air humidity = 25–90%	Laboratory air humidity = 70%
Environmental parameters	Atmosphere	Air humidity = 25–90%	Laboratory air humidity = 70%
	Lubrication	None	None

**Table 3 Materials parameters used to build the selection matrix**

Materials parameters	“Materials” stage thermal, mechanical, and chemical properties	Thermal expansion, thermal conductivity, and critical temperatures (glass transition) Elastic modulus and hardness Chemical composition, corrosion resistance, and residual stresses
	“Process” stage substrate and coating process	Materials machinability, flatness, and roughness Coating thickness and specific requirements for coating process (weight, size, masking, and costs)
	“Couple” stage friction couple	General tribological rules [14], such as assignment of bodies (for example, a body with higher hardness is assigned to the largest kinematic surface) and the coefficient of friction given by bibliography or materials/coatings suppliers

**Table 4** Example of a partial notification tool used for the construction of the selection matrix

Values in the specifications	Weight	Note	1	2	3	4	5
“Materials” stage Contact pressure = 15 MPa Maximal temperature = 150 °C							
Substrate	5	$R_e$ (MPa)	$R_e < 5$	$5 \leq R_e < 15$	$15 \leq R_e < 60$	$60 \leq R_e < 200$	$R_e \geq 200$
Coating	5	$T_{m-s}$ (°C)	$T_{m-s} < 100$	$100 \leq T_{m-s} < 150$	$150 \leq T_{m-s} < 200$	$200 \leq T_{m-s} < 250$	$T_{m-s} \geq 250$
...	5	$T_{m-c}$ (°C)	$T_{m-c} < 100$	$100 \leq T_{m-c} < 150$	$150 \leq T_{m-c} < 200$	$200 \leq T_{m-c} < 250$	$T_{m-c} \geq 250$
“Process” stage Sample geometry/matter Coating process							
Substrate	3	Machinability	Very difficult	Difficult	Good	Very good	Excellent
Coating	4		Not possible on both geometries		Not possible on one geometry		All geometries
...							
“Couple” stage Hardness							
Substrate/coating	2	HV2/HV1	$< 1$		Homogeneous couple		$> 1$
Substrate/coating	1	$\mu$	$\mu > 0.2$	$0.15 < \mu \leq 0.2$	$0.1 < \mu \leq 0.15$	$0.05 < \mu \leq 0.15$	$\mu \leq 0.05$
Friction coefficient (commercial value)							
...							

## 4 Second Phase: Selection Matrix

**4.1 Construction.** A selection matrix is needed to rank frictional couples according to the technical specifications (Table 2) and to find the best solutions. Material and process properties are easily available and stable, while direct tribological characteristics are not numerous and are highly dependent on the experimental device and the procedure conditions.

For the construction of the matrix, the first step is the *categorization of the selection criteria* into three stages (Table 3) which are: a *materials* stage, a *process* stage and a *couple* stage. The distinction between material, process, and couple, i.e., tribological parameters, is useful but artificial: chosen specifications come from tribological considerations, implicitly included in the material response, such as contact pressure or the temperature of the environment.

The second step, when all the parameters are defined, requires the *assignment of a score to each parameter*: 1 = bad performance; 2, 3, 4 = intermediate performance; and 5 = best performance. For most parameters, rating is applied as follows: 1 = very bad response, 2 = bad response, 3 = good response, 4 = very good response, and 5 = excellent response. The choice of the quantitative thresholds separating each grade from 1 to 5 is linked to a relevant material property but also to an implicit tribological performance. However, for binary response, i.e., YES–NO, only 1 and 5 are attributed. Finally, when a parameter is not available for a solution, i.e., when a parameter concerns a coating while the proposed solution is a bulk material, the score 5 is assigned.

The third step establishes the *parameter weights* (between 1 and 5) as a function of their significance. Each score is then multiplied by its weight, and the sum of these weighted scores provides the global score of the solution. The final score is then adjusted to a scale limited to 100.

**4.2 Case Study Application.** This selection matrix can be used as soon as geometry and running conditions are determined. As mentioned above, the first step is to list all the data derived from the specifications (first column of Table 4) and the data related to the substrate or the coating (second column of Table 4).

The second step is to determine the threshold values for each parameter and therefore, to estimate the range value for each parameter. For example, as can be seen in Table 4, the maximum admissible temperature for the application is  $T_m = 150$  °C. Then, score 1 is attributed if  $T_m < 100$  °C; score 2 if  $100 \leq T_m < 150$  °C; score 3 if  $150 \leq T_m < 200$  °C; score 4 if  $200 \leq T_m < 250$  °C; and score 5 if  $T_m \geq 250$  °C. In this example, the median score of 3 was chosen for a target value of 150 °C (maximal environmental temperature) to 200 °C, in order to secure the material choice because of the additional temperature rise due to friction.

Once scores are attributed according to each stage defined in Table 4, the third step is to define the weight parameter. Parameters linked to the materials’ sustainability, like yield strength or maximum admissible temperature, have a high weight, i.e., 5. Parameters whose values are not well known because of their dependence on operating conditions, like the coefficient of friction, have a low weighting, i.e., 1.

Finally, a graphical representation in the form of a polar diagram gives general information about the performance of each solution. The two examples of polar diagrams given in Fig. 3 (Fig. 3(a) for a homogeneous solution and Fig. 3(b) for a heterogeneous solution) are related to parameters defined in Table 4. Other parameters can be used for the construction of the matrix: for this study, 28 parameters (including hardness, corrosion resistance, costs, delivery time...) were used.

In such a graphical representation, the weight of each parameter (defined in Table 4) cannot be considered. However, the score of each parameter with its weight must be added in order to classify all the solutions. The global score can be calculated as follows:

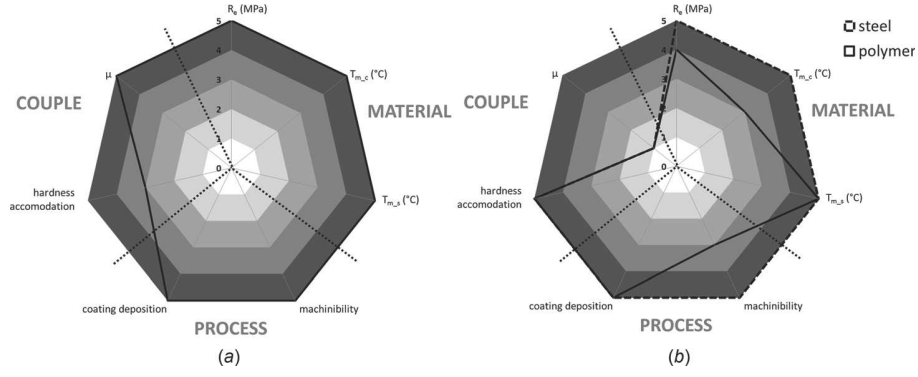


**Fig. 3** Graphic radar drawn from the scores according to the selection matrix: (a) for steel + DLC coating (homogeneous solution) and (b) for polymer (cylindrical bar) against steel (cylindrical-shaped). Dotted lines separate the three stages.

**Table 5** Global scores of the four solutions developed/discussed in this article according to Eq. (1)

Cylindrical-shaped sample	Cylindrical bar	Score
15-5PH steel + DLC coating	15-5PH steel + DLC coating	87/100
15-5PH steel	Reinforced PEEK	81/100
15-5PH steel + PTFE coating	15-5PH steel + PTFE coating	80/100
15-5PH steel	PTFE + mica	79/100

**Table 6** Coating properties

Coating properties	Composition	Microhardness	Thickness ( $\mu\text{m}$ )	Maximum use temperature ( $^{\circ}\text{C}$ )
DLC coating	CrN + a-C:H	2300 HV	2.5	350
PTFE coating	PTFE	—	3–6	220

**Table 7** Mechanical properties of bulk materials (steel and polymer composites)

Mechanical properties	Density ( $\text{kg/m}^3$ )	Hardness	Young's modulus (GPa)	Strength limit (MPa)	Maximum use temperature ( $^{\circ}\text{C}$ )	Thermal conductivity ( $\text{W m}^{-1} \text{K}^{-1}$ )	Coefficient of thermal expansion ( $10^{-6} \text{K}^{-1}$ )
15-5PH steel	$7.8 \times 10^3$	350 HB	196	1060	320	16	10.4
PTFE + mica	$2.06 \times 10^3$	45 HRr	1.2	10	260	0.77	75
Reinforced PEEK	$1.45 \times 10^3$	85 HRm	5.9	78	250	0.78	35

$$\text{global score} = \sum_{i,j,k} (x_i * M_i + y_j * P_j + z_k * C_k) \quad (1)$$

The terms  $x_i$ ,  $y_j$ , and  $z_k$  are the weights of each material parameter  $M_i$ , process parameter  $P_j$ , and couple parameter  $C_k$ . Each solution is analyzed with this selection matrix, and then, the global score for each solution is exhibited. With these scores, it becomes possible to rank all the solutions. This ranking allows the elimination of all the less efficient solutions which show lower scores and the retention of a reduced number of solutions for the experimental tests.

Four solutions will be discussed in this article including bulk polymer composites and coating solutions (Table 5): a DLC coating against the same DLC coating, a PTFE coating against the same PTFE coating, and two polymer composite solutions against uncoated steel.

In general, excellent adherence of the coating to the substrate is crucial. Table 5 is an extract of the overall results obtained with this selection matrix method applied to 35 couples of materials and coatings. According to this extract of the selection matrix, DLC coating sliding against the same DLC coating (Table 5) is one of the best solutions. The key point of this solution is the high

microhardness combined with the flexibility of the coating which is consistent with good wear resistance. For PTFE coating, the key is its self-lubricating properties. The excellent coating adherence on the substrate, due to the process (PTFE is pulverized on the substrate surface), is also advantageous. With regards to the polymer composites, the key factor of the two candidates stems from the additives which are widely used to improve wear resistance, as we will see below.

## 5 Third Phase: Experimental Tests

Using the selection matrix, experimental tests were carried out for 21 solutions. In this paper, we chose to show the results for only four solutions.

### 5.1 Materials and Methods

**5.1.1 Materials.** The four selected solutions, which may potentially improve the life duration of the contact, are detailed as examples. The properties of DLC and PTFE coatings are given in Table 6, while the properties of the three bulk materials, the 15-5PH stainless steel and the two composites, PTFE reinforced with



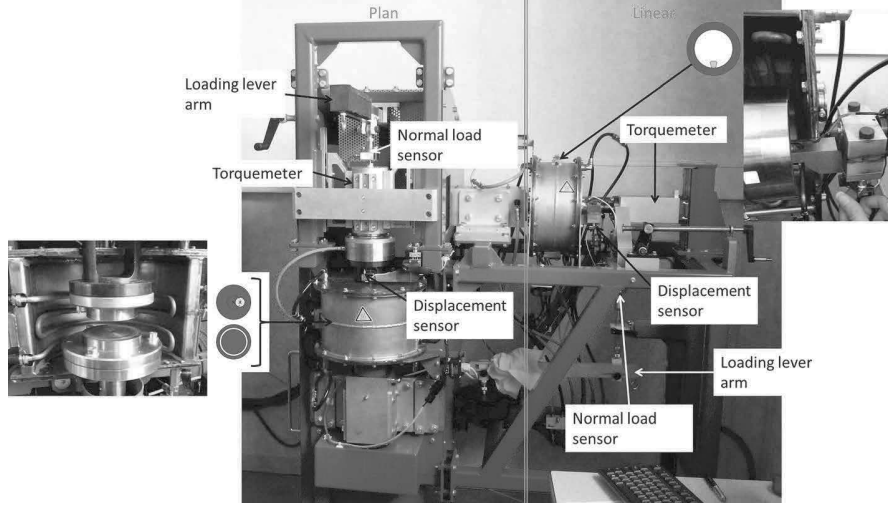


**Fig. 4** General view of the specific tribometer specially designed for this study (plan-on-plan configuration on the left side and linear configuration of contact on the right part)

mica and a PEEK reinforced with graphite, PTFE, and carbon fibers are given in Table 7.

Substrate surfaces are cleaned and degreased before coating. DLC coating is performed by vacuum plasma deposit technology. The roughness of DLC coating is  $R_a = 202 \pm 15$  nm. PTFE coating is obtained by spraying the PTFE. The roughness of PTFE coating is  $R_a = 230 \pm 60$  nm.

**5.1.2 Test Device and Procedure.** A specific tribometer, designed and developed in a collaboration between two French companies, AEREM and PULSWER, and an academic laboratory, LGP (INP-ENIT), was used for the friction tests (Fig. 4), in accordance with the friction conditions observed in the real-life application, that is, temperature, linear speed, contact pressure, and contact geometry. This device allows for several contact configurations: plan-on-plan (ring-on-disk and pin-on-disk) by using the left part of the tribometer, or linear (cylindrical bar-on-cylindrical tub, Fig. 2(b)) by using the right part of the tribometer. For this study, each material or coating solution was tested in each geometrical configuration (linear, pin-on-disk, and annular on disk). However, only the results for the linear configuration are presented in this article.

The normal load is measured by a U2B sensor from HBM (Mennecy, France), characterized by a nominal force of 500 N and an accuracy class of 0.2%. The tangential load is recorded via a T5 torque meter from HBM, with a nominal torque of 20 N·m and an accuracy class of 0.1%. A displacement sensor is supposed to estimate the wear height, but this measurement must be carefully analyzed because this sensor can also simultaneously measure thermal expansion and changes in tribofilm thickness. The contact temperature is estimated with a Pt100 probe located inside the cylindrical bar (fixed sample) 1 mm from the contact surface. The contact temperature is calculated according to the following equation [28]:

$$T_c(t) = T_0 + \frac{T(x, t) - T_0}{\operatorname{erfc}\left(\frac{x}{2\sqrt{at}}\right)} \quad (2)$$

where  $T_c$  is the contact temperature (°C),  $T$  is the measured temperature (°C),  $T_0$  is the ambient temperature (°C),  $t$  is the time (s),  $x$  is the distance between the surface and the position of the temperature probe (m), and  $a$  is the thermal diffusivity of the sample ( $\text{m}^2 \text{s}^{-1}$ ). The difference between the calculated contact temperature and the measured temperature was only a few degrees so the

measured temperature was assumed to be relevant to the mean contact temperature.

The linear configuration has been carried out using a cylindrical bar sliding inside a counter-face cylindrical-shaped sample (Fig. 2(b)). Before the experiments, pressure measurement films (Prescale film by Fujifilm®) control the geometric conformity of the contacting samples. Then, the chamber containing the samples was heated (thermal resistances) to the working temperature ( $\sim 150^\circ\text{C}$ ) for 2 h. This was the time needed to get the samples' temperature to stabilize at  $150 \pm 15^\circ\text{C}$  (the deviation is due to the difference in thermal conductivity). Finally, a mean contact pressure of 6 MPa for polymer-steel contacts and of 15 MPa for coatings-coatings contacts was applied. The friction tests lasted 2 h at a constant sliding speed of  $8 \text{ m s}^{-1}$ . We have not studied the repeatability in this study. So, only one test was performed for each selected solution.

After friction, the wear volumes of cylindrical-shape and cylindrical bar were measured using a WYKO NT9100 (Veeco™, Plainville, NY) optic profilometer. Microscopic observations by scanning electron microscopy (SEM), a ZEISS EVO HD15 (Oberkochen, Germany), were also performed to determine the wear mechanism, and chemical analyses by spectroscopy (or energy dispersive X-ray spectroscopy (EDX)) were carried out to prove whether coatings were partially or totally degraded by friction.

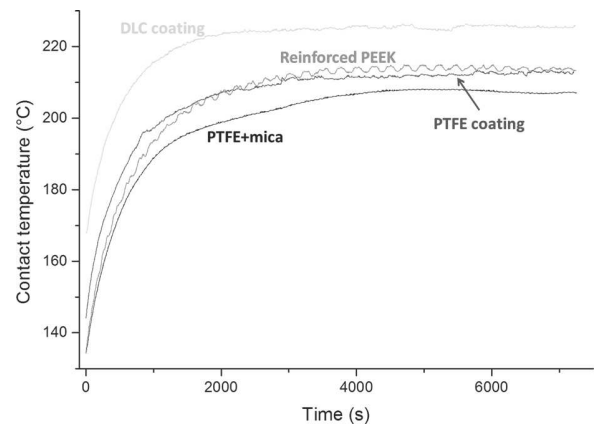


**Fig. 5** Contact temperature,  $T$ , as a function of time and for the four selected materials (sliding conditions:  $150^\circ\text{C}$ ,  $8 \text{ m s}^{-1}$ , 6 MPa for PTFE + mica and reinforced PEEK, and 15 MPa for DLC and PTFE coatings)

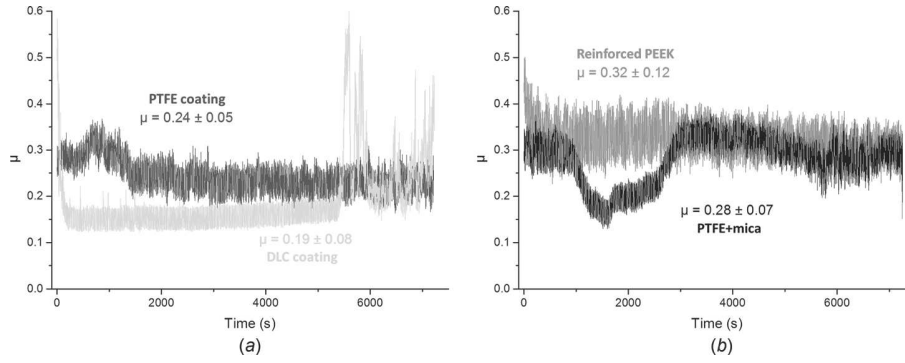


**Fig. 6** Coefficient of friction,  $\mu$ , as a function of time for the four selected materials. (a) DLC and PTFE coatings and (b) PTFE + mica and reinforced PEEK (sliding conditions: 150 °C, 8 m s<sup>-1</sup>, 6 MPa for PTFE + mica and reinforced PEEK, and 15 MPa for DLC and PTFE coatings).

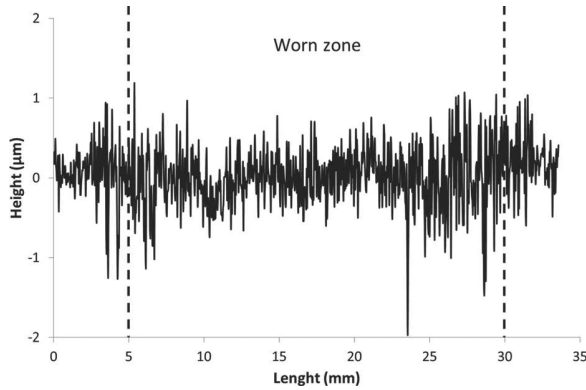


**Fig. 7** Two-dimensional (2D) profile of the worn zone of the cylindrical-shaped sample

## 5.2 Experimental Results

**5.2.1 Temperature Rise.** When sliding began, the contact temperature increased regularly and stabilized after about 2000 s (Fig. 5). For all the solutions, the mean contact temperature was quite similar: between 200 °C (PTFE + mica) and 220 °C (DLC). The temperature rise,  $\Delta T$  (the difference between the contact temperature before friction and the contact temperature at the end of the friction test), varied from 75 °C for DLC to 90 °C for reinforced PEEK. In spite of such high temperature rises, the contact temperature remained below the maximum application temperature for such materials and coatings (Table 6).

**5.2.2 Coefficients of Friction.** The measured coefficients of friction  $\mu$  were broadly stable during the test (Fig. 6). The low value of  $\mu$  for DLC coating at 0.15 illustrates the well-known

self-lubrication effect of DLC layers. However, DLC became unstable and showed a marked increase from 0.18 to 0.55 at the end of the test (Fig. 6(a)). This sharp increase suggests the partial or total degradation of the coating [29]. For PTFE coating (Fig. 6(a)) and reinforced PEEK (Fig. 6(b)), the coefficient of friction was stable during the test. For PTFE + mica, the variation of  $\mu$  at the beginning of the test may have been due to a difficult running-in period. The mean value of  $\mu$  was minimal for DLC ( $0.19 \pm 0.08$ ) and maximal for reinforced PEEK ( $0.32 \pm 0.12$ ).

**5.2.3 Wear Assessments.** Wear volume measurements show that the wear of cylindrical-shaped samples was very low (Fig. 7) and represented about 1% of the total wear, so the total wear was assumed to be only due to the cylindrical bar.

Several 2D wear profiles were extracted from the cylindrical bar (Fig. 8), and the total wear volume was extrapolated to the whole length of the bar. The worn height,  $h$ , was also measured on several 2D profiles. All these measurements are collected in Fig. 9.

Homogeneous coated solutions showed a better resistance to wear when compared to bulk composite polymers sliding against steel (Fig. 9). The coefficients of friction of all the solutions were however very close (Fig. 6). Comparisons using a classical wear rate  $k$ , normalized from wear volume, load, and sliding distance, supported this marked trend (Fig. 10). Regarding the lowest coefficient of friction and the lowest wear rate, DLC coating was confirmed to be a good solution for the tested conditions among the 21 tested sample couples.

**5.2.4 SEM Observations and EDX Analyses.** SEM observations and EDX analyses showed first whether the coating was totally or partially damaged by friction. The initial surface of the DLC coating was composed of a superficial layer of DLC (a-C:H) resting on a sublayer of Si, itself on a thin layer of CrN (Fig. 11). Figure 12 shows an SEM micrograph and its corresponding profile

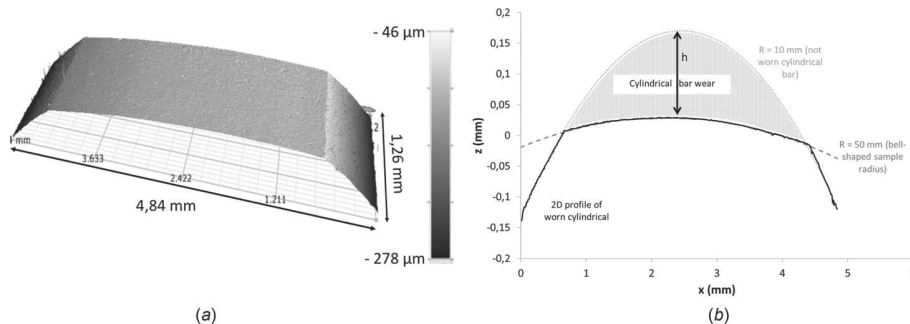


**Fig. 8** (a) Three-dimensional view of a worn cylindrical bar and (b) method for calculation of total wear volume of the cylindrical bar

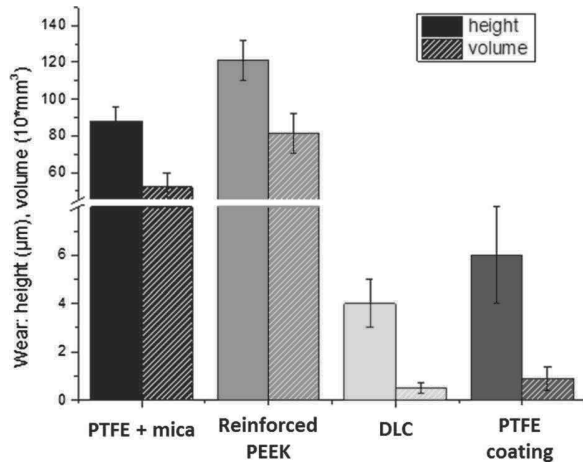


**Fig. 9** Total wear (height and volume) for the four selected materials (sliding conditions: 150°C, 8 m s<sup>-1</sup>, 6 MPa for PTFE + mica and reinforced PEEK, and 15 MPa for DLC and PTFE coatings)

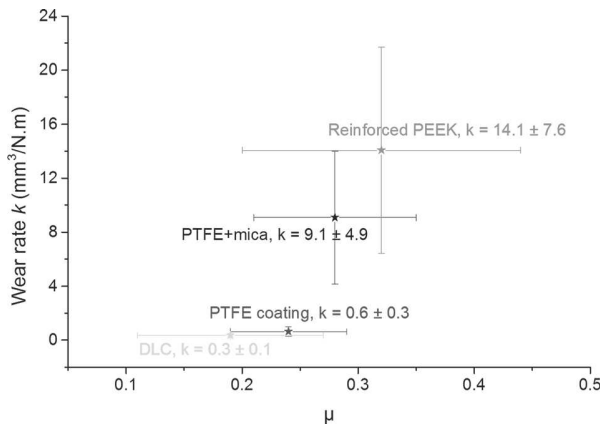


**Fig. 10** Wear rate,  $k$ , as a function of coefficient of friction for tested solutions (sliding conditions: 150°C and 8 m s<sup>-1</sup>)

along a worn and unworn line. The edges of the worn zone showed a drop in concentration for C and presented a wide distribution of Si; DLC was partially damaged, and the Si layer was not damaged. In the center of the worn zone, C and Si were not detected but only Cr and O; this means that DLC was totally damaged and the Cr from the CrN layer was oxidized. However, Fe from substrate was not detected; therefore, the CrN layer was not entirely damaged.

The initial PTFE coating was mainly composed of PTFE (F ~ 40 mass% and C ~ 17 mass%), and a low percentage of aluminum (Al) was detected because the substrate surface was sand-blasted with alumina (Al<sub>2</sub>O<sub>3</sub>) particles before coating deposition (Fig. 13). The low thickness (3–6 μm) of the PTFE coating allowed iron (Fe) from the substrate to be observed on EDX spectra. Figure 14 presents an SEM micrograph, and its corresponding line profile crossing the worn and unworn zones. The PTFE coating was largely damaged in the worn zone: fluorine content was very low (F < 5 mass%), and iron content was higher than in the unworn zone.

Scanning electron microscopy observations also enabled us to determine the wear process. For DLC coating, slight striations revealed a dominating abrasion mode (Fig. 15(a)). Small cracks and local tribofilm pull-out were probably due to a thermal shock during the cooling-off period after sliding. For PTFE coating, the abrasion effect was more marked with larger grooves (Fig. 15(b)).

For reinforced PEEK, the rubbing surface was quite smooth compared to the initial surface, and the chemical composition remained similar when compared to the unworn zones (Fig. 16(a)). In addition, a small amount of metallic debris was observed on the worn track. In contrast, a coarse polymer transfer layer covered the sliding surface of the counter-face 15-5PH steel cylindrical-shaped sample (Fig. 16(b)). This surface morphology pattern characterizes an adhesive wear mode.

For bulk PTFE, the difference of morphology between the worn zone and the unworn zone was relatively slight (Fig. 17(a)). Unlike the reinforced PEEK, the worn zone consisted of a large quantity of debris composed of Mg, Al, Si, S, K, and O (a total of ~15%) corresponding to the composition of mica. As with the reinforced PEEK, a small amount of metallic debris and mica particles was observed on the worn zone, but the polymer tribofilm was not detected on the 15-5PH steel cylindrical-shaped sample (Fig. 17(b)).

**5.2.5 Synthesis of the Results and Discussion.** The expertise was based on different parameters either extracted directly from tests (coefficient of friction and contact temperature) or obtained after characterizing track wear (height of wear, wear rate, composition, wear mechanisms, and amount of free debris) to determine the performance of each tribological solution.

However, when a new product is developed (i.e., innovative air compressor), the lack of references for tribological solutions requires establishing reference values for these parameters from the specifications. Thus, the specifications expressed as thermo-mechanical efficiency, lifetime, or low amount of free debris, for instance, are translated in terms of coefficient of friction ( $\mu_{ref}$ ), power dissipation ( $P_{dref} = \mu \cdot v \cdot F_N$ , where  $v$  is the velocity, and  $F_N$  the normal load), acceptable wear height ( $h_{ref}$ ) without loss of functionality, indicating the wear kinetics ( $W_{kref} = h_{ref}/t$ , acceptable wear height versus time) for bulk materials, and the proportion of worn coating ( $R_{ref} = h_{ref}/h_i$ , ratio between acceptable wear

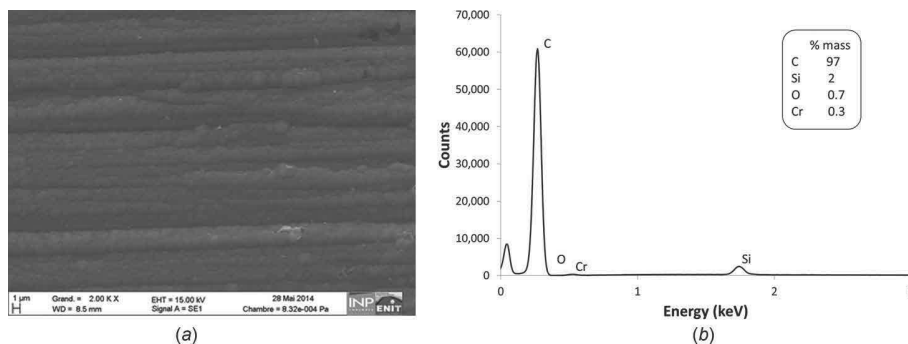


**Fig. 11** SEM analysis of DLC coating on cylindrical bar: (a) image and (b) EDX spectrum of the surface before friction

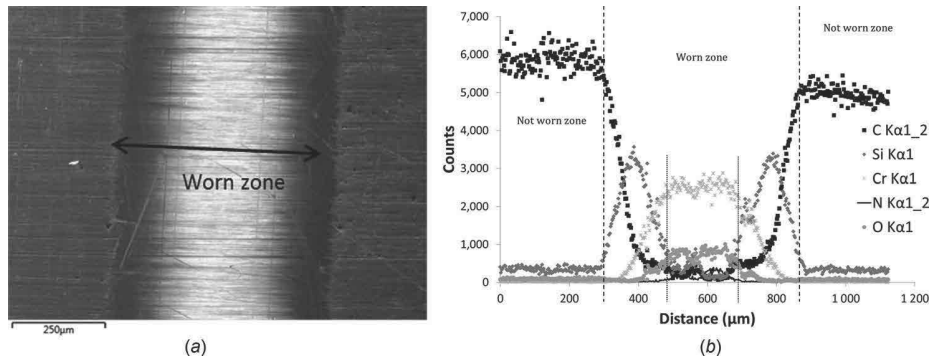


**Fig. 12 SEM analysis of DLC coating on cylindrical bar: (a) image and (b) EDX profile of the worn zone**

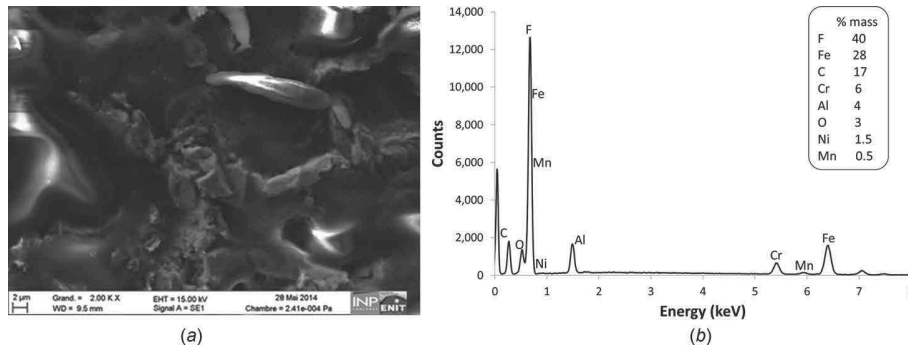


**Fig. 13 SEM analysis of PTFE-based coating on cylindrical bar: (a) image and (b) EDX spectrum before friction**

height and initial thickness of the coating) for coatings, and finally amount of free debris ( $A_{ref}$ ).

As proposed for the preselection phase of material couples, it is also interesting to use a polar representation (graphic radar) to show the synthesis of the results of the tribological expertise. The previously defined parameters are presented as a ratio between the experimental value ( $V_{exp}$ ) and the reference value ( $V_{ref}$ , from the specifications):  $\mu^* = \mu_{exp}/\mu_{ref}$ ;  $P_d^* = P_{d/exp}/P_{d/ref}$ ;  $W_k^* = W_{k/exp}/W_{k/ref}$ ;  $R^* = R_{exp}/R_{ref}$ ; and  $A^* = A_{exp}/A_{ref}$ . These ratios have been established in such a way that a value smaller than one is associated with a performance superior to that of the specification. Thus, the diagram shows the five standard parameters defining the polygon, which materializes their reference value (value of one). This polygon shows two areas: the area inside the polygon is associated with better performances than specifications, while the area outside the polygon illustrates lower performances.

According to the partial selection matrix described above, DLC coating against DLC coating is one of the best solutions, followed by the three other proposed solutions. Experimental tests were run for final selection taking into account tribological properties (Fig. 18). According to our wear rate factor (Fig. 10), DLC coating is the best solution, confirmed by SEM analysis, which showed that the global coating (CrN + Si + DLC) was only partially damaged (Fig. 12). Experimental results confirmed the matrix results. The selection matrix gave the PTFE-based coating and the composite polymers approximately the same ranking. However, experimental results (coefficient of friction and wear rate) set the PTFE coating performance very close to that of the DLC coating (Figs. 10 and 18) when bulk polymers, despite a good coefficient of friction, lead to a high wear volume. This study shows that the selection matrix is able to satisfactorily predict optimal solutions but also demonstrates that an experimental phase remains essential.

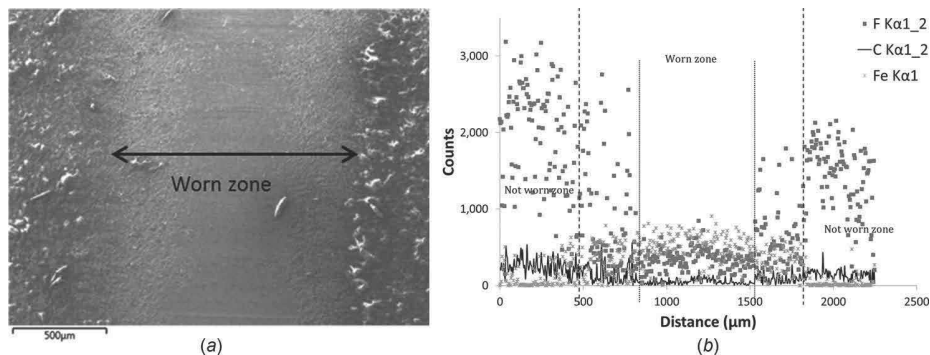


**Fig. 14 SEM analysis of PTFE-based coating on cylindrical bar: (a) image and (b) EDX profile of the worn zone**

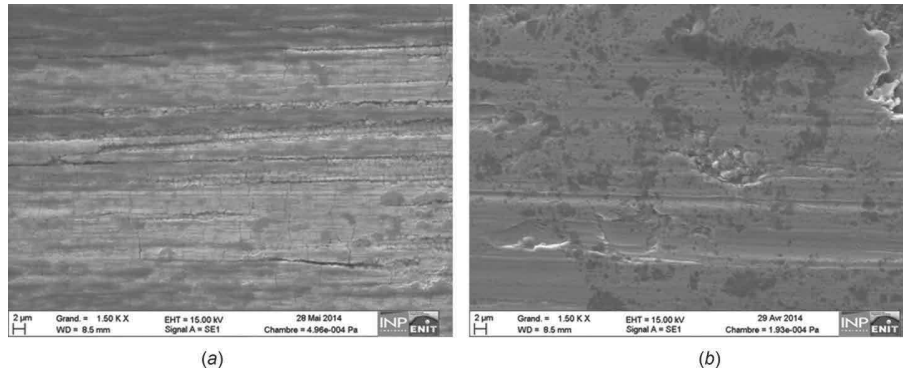


**Fig. 15** SEM images of worn zone of cylindrical bar after 2 h of friction (sliding conditions:  $150^{\circ}\text{C}$ ,  $8\text{ m s}^{-1}$ , and  $15\text{ MPa}$ ) for (a) DLC coating against DLC coating and (b) PTFE-based coating against PTFE-based coating

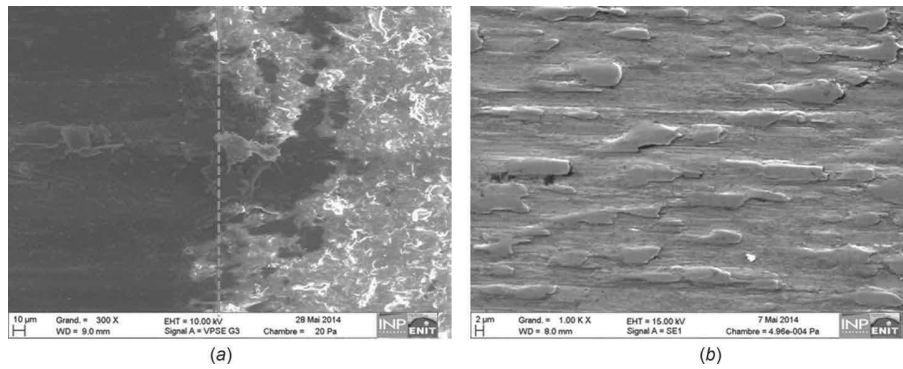


**Fig. 16** SEM images after 2 h of friction of (a) cylindrical bar of reinforced PEEK (worn zone at the left of image) and (b) 15-5PH steel cylindrical-shaped sample (sliding conditions:  $150^{\circ}\text{C}$ ,  $8\text{ m s}^{-1}$ , and  $6\text{ MPa}$ )

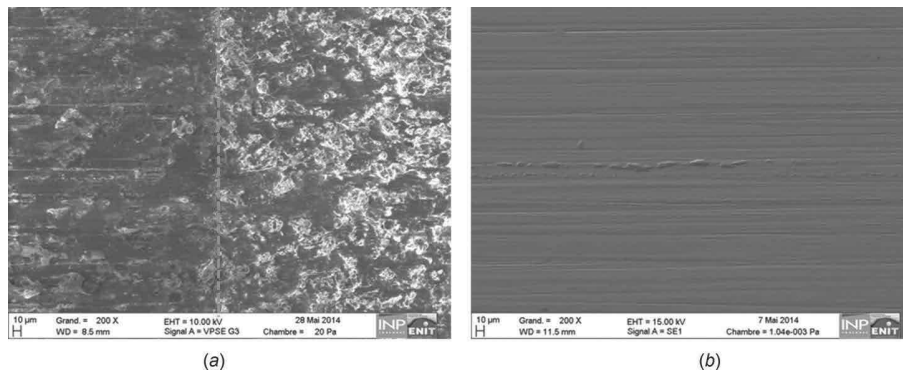


**Fig. 17** SEM images after 2 h of friction of (a) cylindrical bar of PTFE + mica (worn zone at the left of image) and (b) 15-5PH steel cylindrical-shaped sample (sliding conditions:  $150^{\circ}\text{C}$ ,  $8\text{ m s}^{-1}$ , and  $6\text{ MPa}$ )

However, the selection matrix is only based on first bodies data and, even though the working system and the third body are significant factors, they remain largely unknown and cannot be used efficiently in the selection matrix. This may explain why we see a close ranking in the selection matrix, while the experimental results are more widely spaced. These results also raise questions about the relevance of parameters and the weight they are assigned in the selection matrix. For example, in this selection matrix, the parameter *hardness ratio* was given a high weighting. This parameter is the key point for DLC coating, and the drawback for PTFE coating though experimental results is very close for these two solutions. In addition, as might be expected no

correlation could be observed between wear resistance and coating/material hardness ratio concerning this tribological study. Material/coating hardness, in this case, has a lower weight than previously thought. Moreover, some key points, like the self-lubricating property of PTFE, cannot be taken into account in the selection matrix and could distort the ranking.

## 6 Conclusion

This study shows that the selection matrix can be an excellent aid in choosing which solutions would be optimum for a specific tribological study. A three-step procedure is proposed:

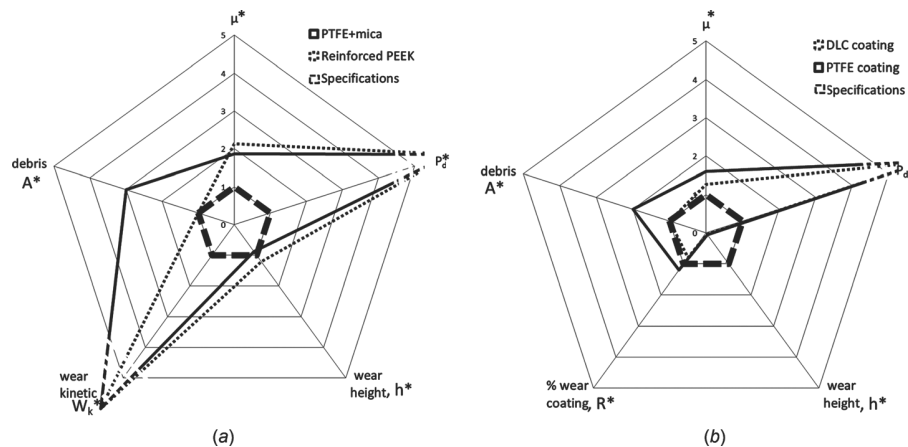


**Fig. 18** Graphic radar representation of experimental results in comparison with expected values from specifications, applied to (a) bulk materials and (b) coatings (sliding conditions: 150 °C and 8 m s<sup>-1</sup>)

- A complete preliminary functional analysis of the contact must be performed. Operational and environmental parameters will give detailed technical specifications.
- A precise construction of the selection matrix is necessary in order to define the best required parameters (materials, process, and couple properties) for the matrix and their relative weight.
- A final experimental phase is essential because several experimental parameters, such as contact stresses imposed by the working system or the formation, composition, and evolution of the third body for a specific contact, cannot be taken into account in the selection matrix. The performance of each solution is highlighted by graphic radar. The last step requires the validation of the optimal selected solutions by experiments on prototypes and finally on a real device.

The case study (an air compressor) is atypical: the geometry is complex, and therefore, it is difficult to have access to all the friction parameters (such as contact pressure and temperature), and friction conditions are severe so it is also difficult to find solutions in the bibliographic data. Despite the lack of data on the real system (compressor prototype) and the third body properties, this selection matrix gave a fairly reliable selection of optimal solutions. The solution with the highest grade/rating was confirmed as a good solution after experimental tests on a tribometer. This solution then had to be confirmed by tests on a prototype.

## Acknowledgment

This research was cofinanced by the European Union and supported by DIRECCTE Midi-Pyrénées. Europe is involved in Midi-Pyrénées (France) through the European Funds for Regional Development.

## References

- [1] Bryant, P. J., Gutshall, P. L., and Taylor, L. H., 1964, "A Study of Mechanisms of Graphite Friction and Wear," *Wear*, **7**(1), pp. 118–126.
- [2] Wei, M. X., Wang, S. Q., and Cui, X. H., 2012, "Comparative Research on Wear Characteristics of Spheroidal Graphite Cast Iron and Carbon Steel," *Wear*, **274–275**, pp. 84–93.
- [3] Li, Y., Ngai, T. L., and Xia, W., 1996, "Mechanical, Friction and Wear Behaviors of a Novel High-Strength Wear-Resisting Aluminum Bronze," *Wear*, **197**(1–2), pp. 130–136.
- [4] Tan, Z. H., Guo, Q., Li, X., and Zhao, Z. P., 2012, "The Tribological Behaviour of Beryllium Copper Alloy QBe<sub>2</sub> Against 30CrMnSiA Steel Under Sliding Condition," *Adv. Mater. Res.*, **399–401**, pp. 2181–2188.
- [5] Buckley, D. H., and Miyoshi, K., 1984, "Friction and Wear of Ceramics," *Wear*, **100**(1–3), pp. 333–353.
- [6] Jia, B.-B., Li, T.-S., Liu, X.-J., and Cong, P.-H., 2007, "Tribological Behaviors of Several Polymer-Polymer Sliding Combinations Under Dry Friction and Oil-Lubricated Conditions," *Wear*, **262**(11–12), pp. 1353–1359.
- [7] Stanford, M. K., and Jain, V. K., 2001, "Friction and Wear Characteristics of Hard Coatings," *Wear*, **251**(1–12), pp. 990–996.
- [8] Mitterer, C., 2014, "PVD and CVD Hard Coatings," *Comprehensive Hard Materials*, Vol. 2, V. K. Sarin, ed., Elsevier, Oxford, UK, pp. 449–467.
- [9] Donnet, C., and Erdemir, A., 2006, "Friction Mechanisms and Fundamental Aspects in Solid Lubricant Coatings," *Materials Surface Processing by Directed Energy Techniques* (European Materials Research Society Series), Y. Pauleau, ed., Elsevier, Oxford, UK, pp. 573–593.
- [10] Godet, M., 1984, "The Third-Body Approach: A Mechanical View of Wear," *Wear*, **100**(1–3), pp. 437–452.
- [11] Luo, D. B., Fridrici, V., and Kapsa, P., 2011, "A Systematic Approach for the Selection of Tribological Coatings," *Wear*, **271**(9–10), pp. 2132–2143.
- [12] Sedlacek, M., Podgornik, B., and Vizintin, J., 2008, "Tribological Properties of DLC Coatings and Comparison With Test Results: Development of a Database," *Mater. Charact.*, **59**(2), pp. 151–161.
- [13] Brechet, Y., Bassetti, D., Landru, D., and Salvo, L., 2001, "Challenges in Materials and Process Selection," *Prog. Mater. Sci.*, **46**(3–4), pp. 407–428.
- [14] Caubet, J.-J., 1964, *Théorie et pratique industrielle du frottement*, Technip, Dunod, Paris.
- [15] Dobrzanski, L. A., and Madejski, J., 2006, "Prototype of an Expert System for Selection of Coatings for Metals," *J. Mater. Process. Technol.*, **175**(1–3), pp. 163–172.
- [16] Athanasopoulos, G., Riba, C. R., and Athanasopoulou, C., 2009, "A Decision Support System for Coating Selection Based on Fuzzy Logic and Multi-Criteria Decision Making," *Expert Syst. Appl.*, **36**(8), pp. 10848–10853.
- [17] Franklin, S. E., and Dijkman, J. A., 1995, "The Implementation of Tribological Principles in an Expert-System (PRECEPT) for the Selection of Metallic Materials, Surface Treatments and Coatings in Engineering Design," *Wear*, **181–183**(1), pp. 1–10.
- [18] Streiff, R., 1993, "Databases and Expert Systems for High Temperature Corrosion and Coatings," *Corros. Sci.*, **35**(5–8), pp. 1177–1187.
- [19] Syan, C. S., Matthews, A., and Swift, K. G., 1987, "Knowledge-Based Expert Systems in Surface Coating and Treatment Selection for Wear Reduction," *Surf. Coat. Technol.*, **33**, pp. 105–115.
- [20] Schiffmann, K., Petrik, M., Fetzer, H. J., Schwarz, S., Gemmler, A., Griepentrog, M., and Reiners, G., 2002, "INO-A WWW Information System for Innovative Coatings and Surface Technology," *Surf. Coat. Technol.*, **153**(2–3), pp. 217–224.
- [21] Matthews, A., Holmberg, K., and Franklin, S., 1993, "A Methodology for Coating Selection," *Tribol. Ser.*, **25**, pp. 429–439.
- [22] Matthews, A., Franklin, S., and Holmberg, K., 2007, "Tribological Coatings: Contact Mechanisms and Selection," *J. Phys. D: Appl. Phys.*, **40**(18), pp. 5463–5475.
- [23] Langlade, C., Vannes, B., Taillandier, M., and Pierantoni, M., 2001, "Fretting Behavior of Low-Friction Coatings: Contribution to Industrial Selection," *Tribol. Int.*, **34**(1), pp. 49–56.
- [24] Luo, D. B., Fridrici, V., and Kapsa, P., 2010, "Selecting Solid Lubricant Coatings Under Fretting Conditions," *Wear*, **268**(5–6), pp. 816–827.
- [25] Liskiewicz, T., Fouvry, S., and Wendler, B., 2005, "Development of a Wöhler-Like Approach to Quantify the Ti(C,N)<sub>2</sub> Coatings Durability Under Oscillating Sliding Conditions," *Wear*, **259**(7–12), pp. 835–841.
- [26] Carton, J.-F., Vannes, A.-B., and Vincent, L., 1995, "Basis of a Coating Choice Methodology in Fretting," *Wear*, **185**(1–2), pp. 47–57.
- [27] Cartier, M., and Kapsa, P., 2001, "Usure des contacts mécaniques—Éléments de tribologie," *Techniques de l'Ingénieur Frottement et Usure*, Editions T. I., Paris, Ref. Article, BM5066, pp. 1–13.
- [28] Foulon, D., Watremez, M., Bricout, J.-P., and Oudin, J., 1995, "Caractérisation thermomécanique de disques de frein ferroviaires multimatériaux," *Matér. Tech.*, **83**(10–11), pp. 3–12.
- [29] Ronkainen, H., Varjus, S., and Holmberg, K., 1998, "Friction and Wear Properties in Dry, Water- and Oil-Lubricated DLC Against Alumina and DLC Against Steel Contacts," *Wear*, **222**(2), pp. 120–128.